ORIGINAL ARTICLE

Investigation on the role of preform architecture on the property performance of recycled cotton-based engineered eco-composites

Zunjarrao Kamble[1,2] · Bijoya Kumar Behera[2]

Abstract

This research used cotton fibres extracted from waste textiles (shoddy) and cotton shoddy-based yarn to produce nine distinct preforms. This study aims to develop different preform architectures using cotton shoddy web, cotton shoddy-based yarn, and their epoxy composites for different applications. The developed composite's mechanical, thermogravimetric, and water absorption properties were characterised for understanding their applicability in structural materials. The composites with cotton shoddy web sandwiched between waste cotton yarn-based unidirectional structures (WbUD) have ~ 26 and ~ 72% higher flexural and izod impact strength than composite reinforced with cotton shoddy web (SH) alone. Meanwhile, the tensile strength of SH and WbUD was approximately the same. Compared to SH, the composites with a cotton shoddy web sandwiched between woven fabrics made of waste cotton yarns (WbUD) do not exhibit enhancement in mechanical properties. The composite with cotton web sandwiched between hybrid woven fabrics has tensile, flexural, and izod impact strengths of 74, ~ 68, and ~ 537% higher than SH. The composite laminates exhibit notably lower equilibrium water content than SH. The developed composites are green materials and can be used to produce various components for building and construction, furniture materials, and automotive applications.

Keywords Eco-composite · Upcycling · Structural composite material · Compression moulding

1 Introduction

Natural fibre-reinforced composites are growing due to their environmental and economic benefits. However, in some applications, the mechanical properties of composites desired for a particular application can be met using alternative raw materials such as fibres extracted from waste textiles. This ultimately reduces the dependency on natural fibres whilst saving environmental resources and costs. Further, textile waste is increasing globally due to the increment in per capita consumption and population; therefore, it is abundantly available. The per capita consumption of textiles doubled in 2013 compared to 1992 [1]. The total fashion waste will be 148 million tons by the end of 2030, and an estimated 150 million tons of clothing will be landfilled in 2050 [2].

Four ways to reinforce composites using waste textiles are using waste textiles in fabric form, mechanical shredding to fibrous form (shoddy), developing various textile structures using shoddy as the base material and textile waste-based nano or microstructures as filler in composites [3–5]. Dissanayake and Weerasinghe [6] reported that cotton and cotton/polyester blended textiles are the most studied textiles for recycling. In another study, Dissanayake et al. [7] developed thermal insulation panels via compression moulding using nylon/spandex and polyurethane-cutting waste generated in garment manufacturing. They found that the 60% nylon/spendex shred insulation panel and 40% polyurethane exhibited the best thermal insulation. Zhang et al. [7] developed waste cotton linter-based composite hydrogels for dye removal. Ramamoorthy et al. [8] reported cotton/polyester (50:50) plain-weave fabrics reinforced acrylated epoxidized soybean oil-based laminated composite materials. They concluded that tensile strength and modulus of over 100 MPa and 10 GPa can be obtained without fabric

✉ Zunjarrao Kamble
  kamblezb@nitj.ac.in

1 Department of Textile Technology, Dr B R Ambedkar National Institute of Technology Jalandhar, G.T Road, Amritsar Bypass, Jalandhar 144008, Punjab, India

2 Department of Textile and Fibre Engineering, Indian Institute of Technology Delhi, Hauz Khas, New Delhi 110016, Delhi, India

treatment. Temmink et al. [9] also reported the same kinds of stacked laminates using denim waste. Further, Owen et al. [10–12] in their experiments, recycled glass fibre and polypropylene to produce compression moulded composite products. Their study reveals that the glass fibre-reinforced polypropylene composites can be recycled three times; after that, mechanical properties deteriorate. This is mainly due to the reduction in glass fibre length and molecular weight of polypropylene. Further, in another study, Owen et al. [13] reported higher thermal degradation temperature of epoxy-coated silane-treated kenaf fibres reinforced with recycled PET composites and stated that these composites could be used for high-temperature industrial applications. Singh et al. [14] reported polyester composites reinforced with rice husk waste and seashells and concluded that the developed composites could be used for structural components of an automobile. Hangargi et al. [15] developed Kevlar-polypropylene composites filled with cotton stalk powder and reported enhancement in the composite's mechanical and dynamic mechanical properties. Jagadeesan et al. [16] reported enhancement in tensile, flexural, and impact properties of polyester composites reinforced with banana and basalt fibre and filled with cellulose derived from sesame oil cake. They also concluded that adding cellulose derived from sesame oil cake in the composite helps enhance load transfer from the matrix to the fibre.

Further, some studies reported composites reinforced with preforms developed using waste textiles. Many of these studies report composites reinforced with nonwoven fabric made from shoddy [17–19]. However, very few studies have reported woven preforms made from waste textiles. Umar et al. [3] reported cotton preform made using a virgin cotton warp and weft yarn from noil and knitting waste. Using the produced fabric, they used a vacuum-assisted resin infusion technique to produce laminated composites. Frydrych et al. [20] reported plain woven cotton and jute preform produced using yarn made of waste cotton and jute fibres.

Almost all the reported research on textile waste-reinforced composites revolves around composites made from waste fabrics, composites made from shoddy, and composites loaded with nano/microstructures produced using waste textiles. Of these four techniques, composites reinforced with the textile preforms made of woven fabric using shoddy-based yarn are rarely reported. Further, no study reported engineered laminates made of shoddy web and woven fabric made of recycled cotton yarns. Combining waste textiles with high-strength fibres can substantially improve the composite's mechanical properties. However, only one study is known to the authors where an epoxy composite was reinforced with a laminate of the waste cotton web and glass mat. The textile waste-reinforced composites can produce mechanical properties desired for furniture materials, door-filling materials, flooring underlayment, packaging, etc.,

provided this waste is arranged in a proper preform structure [21]. Engineering the preform structure can enhance the mechanical characteristics of textile waste-based composites. This research reports nine distinct novel preform structures produced using waste textiles and their composites. The compression moulding technique was employed in this research to develop the composite specimens with a 0.3-fibre volume fraction. The developed composites were characterised by their mechanical and thermogravimetric properties and compared with commercially available materials.

2 Materials and methods

2.1 Materials

Recycled cotton fibres derived from textile waste were employed as reinforcement material. A rag-tearing (shredding) machine was used to shred the cotton textile waste. The shredding machine shreds the discarded fabric pieces into a fibrous form termed 'Shoddy'. The mechanical shredder fails to open hard twisted fine yarns to the fibre state; consequently, they remain unopened or partially opened in the shoddy (Fig. 1). Wanassi et al. [22] reported two equations to determine the weight yield of fibres within the shoddy. However, they did not mention the procedure for the same. Further, no test standard is available for measuring the quantity of fibres and unopened yarns within the shoddy. Therefore, ten shoddy samples weighing 100 mg each were
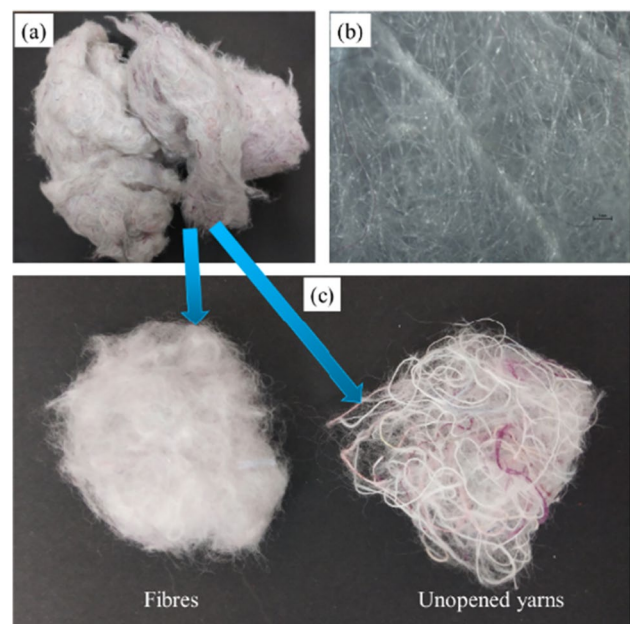
Fig. 1 Cotton shoddy (**a**) and its microscopic view (**b**), fibres, and unopened yarns within the shoddy (**c**)

randomly picked from the bulk to assess the weight percentages of fibres and unopened yarns inside the shoddy. The fibres and unopened yarns within the shoddy were separated manually and weighed to estimate the proportion of

fibres and unopened yarns. It has been observed that the shoddy comprises ~ 80% completely opened fibres and ~ 20% unopened or partially opened yarns. Equations (1) and (2) are used to determine the percentage of fibres and unopened yarns within the shoddy [22].

$$W_f(\%) = \frac{W_s - W_y}{W_s} \times 100 \tag{1}$$

$$W_y(\%) = 100 - W_f(\%) \tag{2}$$

where W_s, W_f, and W_y are the weights of shoddy, fibres within shoddy, and yarns within shoddy, respectively.

The rotor-spun shoddy yarn with an average linear density of 476 ± 4 tex (~ 90% cotton fibres, and ~ 10% other fibres extracted from waste fabrics) was used to produce woven preforms (Fig. 2). The rotor-spun yarn was procured from the local market in India, and its optical microscopic image is shown in Fig. 3c. The typical load-strain curve of the waste cotton yarn is shown in Fig. 1S (Supplementary material). A 600-tex glass yarn procured from Owens Corning
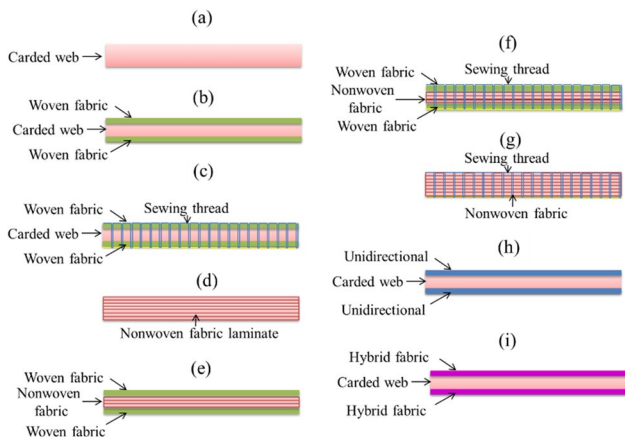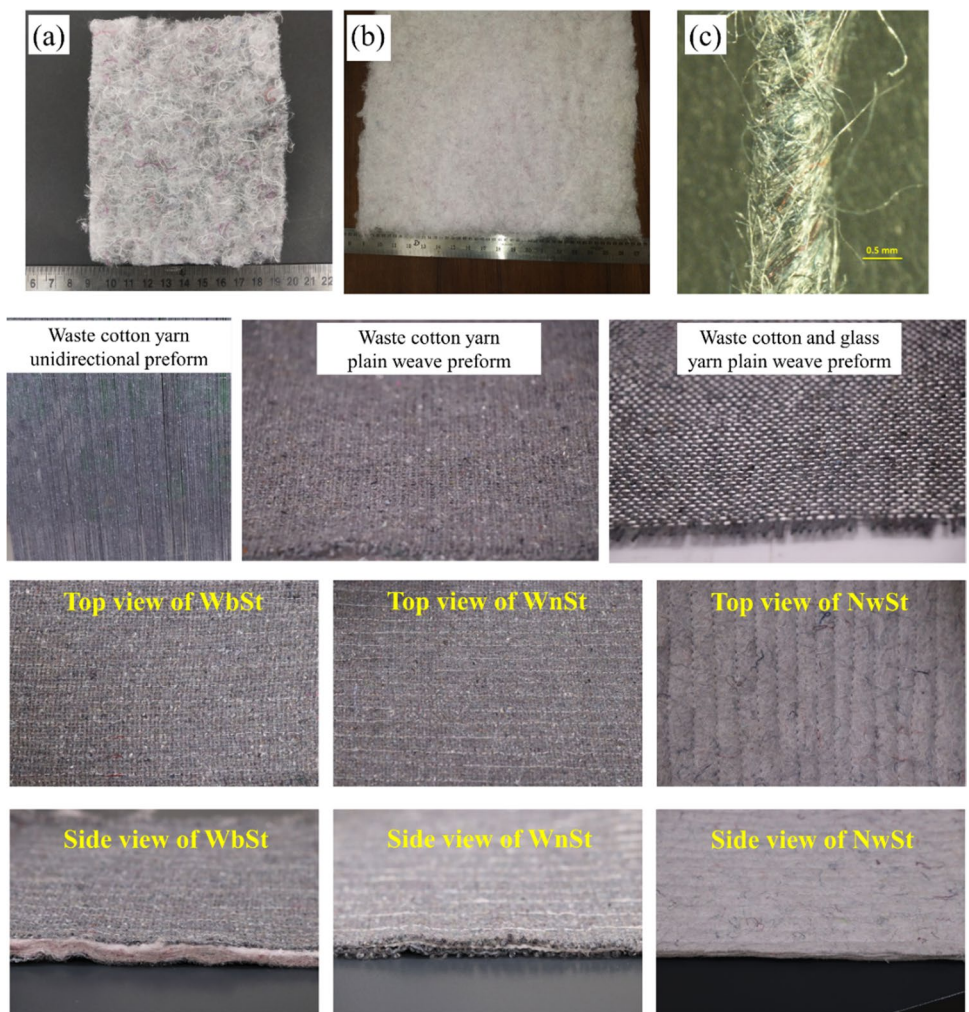

Fig. 2 Line diagram of different preforms

Fig. 3 Single-layer (**a**) and multi-layer (**b**) carded shoddy web, shoddy yarn-based different fabric structures, and photographs of top and side view of different stitched preforms

Ltd., India was used for producing a plain weave hybrid fabric with waste cotton rotor-spun yarn as warp. Table 1 shows cotton fibre's physical and mechanical properties, waste cotton rotor-spun yarn, and glass yarn. Polyester/cotton thread with a 75 ticket number was used to stitch the preforms. The stitching thread was procured from the local market. The epoxy resin Lapox ARL125 and its curing agent, AH365, were provided by Atul India Ltd. Table 1S (Supplementary material) shows the properties of the resin and its curing agent.

2.2 Production of textile waste-based preform architectures

To improve the mechanical characteristics of their composites, the preforms produced in this work are a mix of woven textiles and cotton web or nonwoven. Shoddy cotton carded web, shoddy cotton nonwoven, and three woven fabric structures created from waste cotton yarn were developed as textile waste-based structures. A carding machine was used to create a multi-layer fibre web from the shoddy cotton fibres. Based on the author's past research, a 200 m/min carding speed was chosen [23]. The areal density of a single layer of the carded web was maintained at ~27 g/m^2. On the DILO needle punching machine, a shoddy cotton nonwoven with an area density of 200 g/m^2 was produced with a needle punch density of 150 punches per square inch. Three distinct types of woven fabric structures were developed (Fig. 3). Table 2 lists the specifications of the developed woven fabrics. The unidirectional (UD) structure was produced by laying waste cotton rotor yarns parallel and maintaining constant yarn spacing. Two distinct plain

weave fabrics were developed—all waste cotton rotor-spun yarn and hybrid fabric having waste cotton yarn as warp and glass yarn as weft. These fabrics were woven on a sample weaving machine (make: Dynamic Looms, India) (Fig. 2S supplementary material).

Nine different types of preforms were developed for composite preparation as detailed below:

(1) Carded cotton shoddy web (SH): A pre-calculated quantity of a carded cotton shoddy web was used to develop a composite specimen (Fig. 2a).
(2) Cotton nonwoven (Nw): A laminated cotton shoddy nonwoven preform (preform size as per mould dimensions) has the desired weight according to the required fibre volume fraction (Fig. 2d).
(3) Stitched cotton nonwoven (NwSt): The cotton nonwoven fabric was cut in line with the mould dimension (30 × 30 cm). The pre-calculated quantity of cotton nonwoven, having dimensions in line with mould, was taken. These nonwoven fabrics were stacked and stitched. The preform was stitched with a 75-ticket-number polyester sewing thread on the Juki lockstitch sewing machine. The stitch length was kept at 5 mm. The stitch lines were maintained 1 cm apart (Figs. 2g and 3). These stitch parameters were kept constant for all the stitched preforms.
(4) Cotton web sandwiched between woven fabrics (Wb): The plain weave fabric made of all waste cotton yarn was cut in line with the mould measurements and weighed. During composite manufacturing, the fibre web was sandwiched between woven fabrics (Fig. 2b).
(5) Cotton web sandwiched between woven fabrics and stitched (WbSt): A preform having a cotton web sandwiched between woven fabrics was developed and stitched (Figs. 2c and 3).
(6) Nonwoven sandwiched between woven fabrics (Wn): The preform Wn is similar to Wb. Unlike carded web in Wb, in Wn, the nonwoven fabric is sandwiched between woven fabrics (Fig. 2e).
(7) Nonwoven sandwiched between woven fabrics and stitched (WnSt): This preform is similar to WbSt (Figs. 2f and 3).
(8) Cotton web sandwiched between UD fabrics (WbUD): The preform WbUD consists of the skin of unidi-

Table 1 Properties of the cotton fibre, waste cotton yarn, and glass multifilament yarn

Description	Cotton fibre	Waste cotton rotor-spun yarn	Glass multifilament yarn
Length (mm)	18 ± 2	Continuous	Continuous
Diameter/thickness (µm)	11 ± 1	810 ± 26	186.5 ± 0.4
Tensile strength (MPa)	167 ± 14	26.9 ± 5.5	723.5 ± 54
Modulus (GPa)	4.5 ± 0.5	2.07 ± 0.4	19.52 ± 1.4
Elongation (%)	5 ± 0.4	16.45 ± 2	4.16 ± 0.6

Table 2 Woven fabric specifications

Preform	Unidirectional preform	Plain weave fabric with all waste cotton yarn	Plain weave hybrid fabric (warp, waste cotton yarn; weft, 600-tex glass yarn)
Ends per inch	24	12	12
Picks per inch		12	10
Areal density (gm/m^2)	~450	~450	~450

rectional fabric of waste cotton yarn-based structure (Fig. 2h).

(9) Cotton web sandwiched between hybrid woven fabrics (WbH): The plain weave hybrid fabric having waste cotton yarn as warp and cotton shoddy-based yarn as weft was used as preform skin (Fig. 2i).
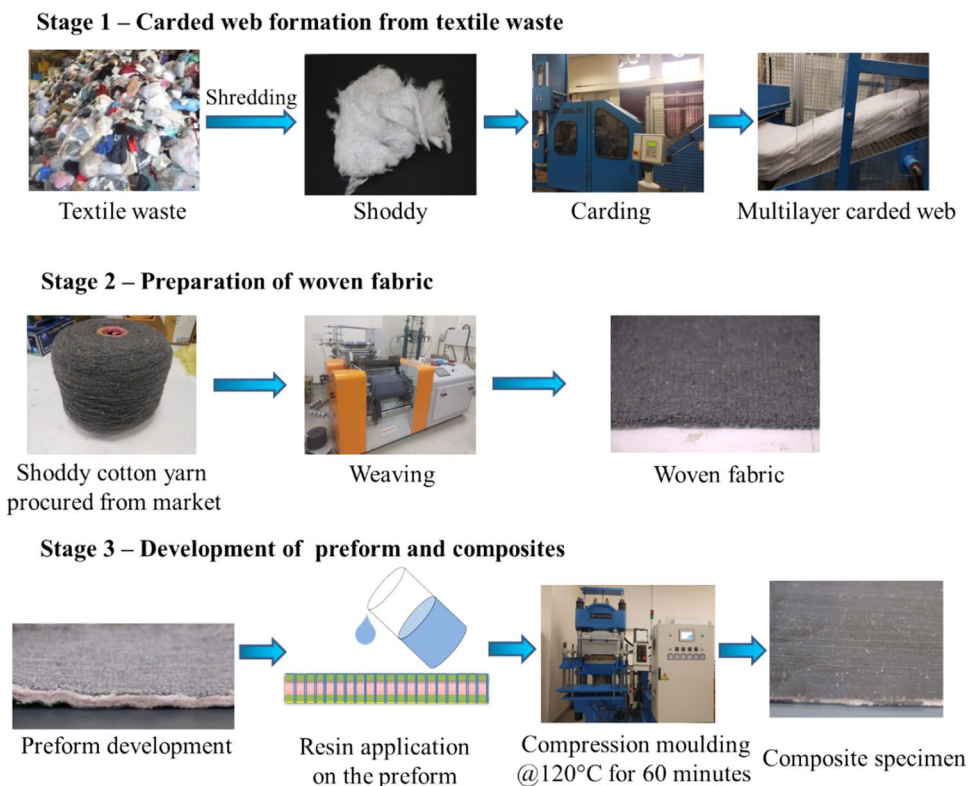
2.3 Composite specimen development

The scheme of composite development is shown in Table 3, and the composite development process is depicted in Fig. 4. A stainless steel mould having dimensions 30 × 30 × 0.3 cm was taken. The weighed quantity of epoxy matrix and hardener in the ratio of 100:32 were mixed in a beaker with a glass rod, followed by degassing. The resin was applied uniformly to the preform by placing it into the mould. The mould was then covered with a Teflon sheet and shifted to a compression moulding machine preheated to 120 °C. All the composites were cured for 60 min. The curing time and temperature were chosen according to the resin supplier's guidelines. The fibre volume fraction and thickness of developed composite specimens were maintained at ~0.3 and ~3 mm, respectively.

Table 3 Scheme of composite development

Sample ID	Preform type	Woven fabric weight (%) in the composite	Web/nonwoven weight (%) in the composite	Matrix weight (%) in the composite
SH	Carded cotton web		38	62
Nw	Cotton nonwoven laminate		38	62
NwSt	Stitched cotton nonwoven laminate		38	62
Wb	Cotton web sandwiched between woven fabrics	26.33	10.37	63.3
WbSt	Cotton web sandwiched between woven fabrics and stitched	26.7	9.3	64
Wn	Nonwoven sandwiched between woven fabrics	26.07	9.93	64
WnSt	Nonwoven sandwiched between woven fabrics and stitched	25.85	10.99	63.16
WbUD	Cotton web sandwiched between UD preform	23.24	14.45	62.43
WbH	Cotton web sandwiched between hybrid woven fabrics	26.79	8.93	64.28

Fig. 4 Composite laminate development process

Stage 1 – Carded web formation from textile waste

Textile waste → Shredding → Shoddy → Carding → Multilayer carded web

Stage 2 – Preparation of woven fabric

Shoddy cotton yarn procured from market → Weaving → Woven fabric

Stage 3 – Development of preform and composites

Preform development → Resin application on the preform → Compression moulding @120°C for 60 minutes → Composite specimen

2.4 Characterisation of the composite specimens

Tensile characteristics of the composite specimens were determined using ASTM D3039 standards, flexural properties using ASTM D7264 standards, and izod impact strength using ISO 180:2000 standards. The bearing strength of the composite in a double-lap pinned joint without any torque to the fastener was characterised according to ASTM D5961. The test fixture is shown in Fig. 3S (Supplementary material). The mechanical tests are detailed in Table 2S (Supplementary material). The ASTM D570 standard was used to determine the composite's water absorption properties. Numerous aspects of water absorption, such as equilibrium water content, diffusion coefficient, water transmission rate, absorption coefficient, and permeability coefficient, have been estimated and analysed. The same details are shown in Table 3S (Supplementary material). The thermal conductivity of the produced composites was determined using a PerkinElmer TGA 400 thermogravimetric analyser. Composite specimens weighing less than 10 mg were exposed to temperatures ranging from ambient temperature to 600 °C with increments in temperature at a constant rate of 20 °C per minute in an N_2 atmosphere. Five specimens were characterised each for tensile, flexural, izod impact strength, water absorption study, and thermogravimetric analysis. The tensile and impact-cracked surfaces were examined using a scanning electron microscope (SEM) (Zeiss EVO18) to study the composite's failure mechanisms and fibre-matrix interface.

3 Results and discussion

3.1 Mechanical properties of the composites

As shown in Table 4, the average tensile strength and Young's modulus of all the composites except WbH are lower than the composite specimen SH by 43% and 17%.

Composite specimens such as Wb, Wn, WbSt, and WnSt have a lower tensile strength because woven fabric occupies 72% of the total reinforcement weight within the preform, and only half of the threads within this woven preform are in a loading direction. There are differences between the structure of preform WbUD and SH, though. All of WbUD's skin layers have yarns running in the same direction as the load, so the tensile strength of the composite is almost identical to SH. Its Young's modulus is 73% greater than SH. When tensile stress is applied to the WbUD composite, the outer layer, which has a higher modulus than the core material (due to the unidirectional yarn arrangement), first bears the stress conveyed via the matrix. The load is transmitted to the cotton/epoxy core when the outer layer fractures, and the entire composite collapses when the applied stress exceeds the bearing stress of the cotton/epoxy core. Due to the improved contact between the layers, the composite's tensile strength was enhanced after sewing. The tensile strength of WbSt and WnSt composite specimens is 14 and 8% greater than Wb and Wn composites, respectively. The Wb and Wn composites have approximately identical tensile strengths. WbSt, Wb, WnSt, and Wn all have the same Young's modulus. Furthermore, the NwSt composite has an 8% greater tensile strength and a 9% higher Young's modulus than the Nw composite.

The composite specimen Nw shows 5% lower tensile strength than the composite specimen SH. This demonstrates that needle punching the shoddy web does not help to enhance the tensile strength. This can also be ascribed to the nonwoven's decreased fibre extent due to needle punching [24]. The composite specimen WbH, consisting of high-strength glass yarn in the loading direction, shows 74% higher tensile strength and 183% higher Young's modulus than SH. When glass yarn within the composite specimen WbH fractures, the matrix transfers stress to the cotton fibres, which causes them to fail when the applied stress

Table 4 Mechanical properties of different types of composites

Specimen ID	Tensile strength (MPa)	Elongation at break (%)	Young's modulus (MPa)	Flexural strength (MPa)	Flexural modulus (MPa)	Izod impact strength (KJ/m^2)
Neat epoxy	59.9 ± 2.64	4.9 ± 0.4	2494.67 ± 114	70.86 ± 1.28	2724.52 ± 145	4.18 ± 0.6
SH	80.54 ± 0.26	5.52 ± 0.5	2944.03 ± 322	85.75 ± 0.68	5913.7 ± 310	6.48 ± 0.2
Nw	76.8 ± 3.61	5.44 ± 0.3	3288.67 ± 288	87.62 ± 2.30	5688 ± 226	8.6 ± 0.3
NwSt	83 ± 1.8	4.82 ± 0.3	3590 ± 25	87.48 ± 1.2	5530.7 ± 120	9.09 ± 1.4
Wb	53.49 ± 0.97	4.1 ± 0.4	2472.27 ± 19	58.63 ± 0.5	3651.1 ± 385	9.17 ± 0.1
WbSt	60.78 ± 1.73	4.62 ± 0.35	2507.79 ± 3	59.9 ± 0.2	3720.2 ± 25.8	9.34 ± 0.5
Wn	53.42 ± 0.52	4 ± 0.3	2479.96 ± 41	58.63 ± 1.9	3425.2 ± 165	9.55 ± 1.1
WnSt	57.91 ± 0.22	4.3 ± 0.01	2531.92 ± 13	57.91 ± 0.2	3475.3 ± 12.9	9.3 ± 0.6
WbUD	78.39 ± 1	2.74 ± 0.27	5093.38 ± 348	107.76 ± 3.37	10,277.84 ± 284	11.14 ± 0.92
WbH	140.2 ± 2.09	2.99 ± 0.01	8325.29 ± 57	143.54 ± 4.9	9365.4 ± 34.2	41.26 ± 4.4

exceeds the breaking stress of the cotton web/epoxy at the core.

WbH composite has 79% greater tensile strength and 63% higher Young's modulus than WbUD composite. Figure 5a shows the stress–strain curves of several composites. Figure 6 shows SEM images of tension-fractured composite specimens SH and Wb. Fibre matrix debonding, fibre pullout, and fibre fracture are the primary causes of failure in the composite specimen SH. The cotton fibre's main wall split, leaving the secondary wall stretched under the tensile stress conveyed to the fibre through the matrix, as seen in Fig. 6a and b. Cotton fibre fracture, fragmentation of cotton fibre during a break, fibre pullout, and fibre-matrix debonding are shown in Fig. 6c and d. Figure 6e shows that the composite specimen Nw fails due to fibre matrix debonding, fibre pullout, fibre fracture, and non-woven layer delamination. In a composite specimen, Wb, the woven fabric's debonding outer layer and the carded web were observed (Fig. 6f). Further, Fig. 6g and h depicts that the epoxy matrix thoroughly wets the woven fabric's yarns. The composite specimen WbH fails catastrophically, which may be due to a very high difference in the modulus of glass yarn and cotton fibre. SEM image of tensile fractured WbH composite shows glass fibre and epoxy debonding (Fig. 7). However, cotton fibre pullout is also observed mainly due to poor cotton and epoxy interfacial strength (Fig. 7c).

The composite laminate's average flexural strength and flexural modulus, namely Wb, Wn, WbSt, and WnSt, are 40 and 66% lower than the SH composite. Under three-point bending, the top side of the composite gets compressed, and the bottom side tensioned. The fibre type and orientation of the composite laminate skin determine the flexural strength and stiffness of the composite [25]. Wb, Wn, WbSt, and WnSt composite laminates have less flexural strength because the woven fabric layer at the tension side of each laminate starts to break down early. This causes the laminates to be less strong [26].

Compared to SH, the flexural strength and modulus of the WbUD composite increase by 26% and 74%, respectively, when UD preform is used as the skin layer. In the case of WbUD, all threads inside the skin layer contribute to load-bearing. For plain weave preforms, only half of the preform's fibres can support the flexural load developed on the bottom side. The high flexural strength of the composite specimen WbH is due to the presence of high-strength glass fibres on the skin. The composite specimen WbH has a flexural strength of 68% greater than SH. Although laminated composite experiences low stress at the outer layer, it fails due to yarn breakage. The core fails to support the bottom skin due to poor interface caused by the difference in the size of cotton fibre at the core and yarn at the skin. Further, no notable difference between stitched and unstitched preform reinforced composite's flexural strength was observed.

Similarly, SH, Nw, and NwSt composites did not differ in flexural strength. High-strength glass fibre's presence increases the resistance to shearing in composite specimen WbH, which results in its high flexural strength. The flexural strength of composite specimen WbH is ~68% higher than SH. The fractured composite specimens SH, Wb, and WbH are shown in Fig. 8.

When a composite specimen is subjected to impact loading, the impact strength is the amount of energy required to shatter it. Overall toughness, which results from materials, fibre-matrix interface, construction, composite geometry, and test methods, governs the composite's impact strength [27]. Composite specimens Wb, Wn, WbSt, and WnSt have a 40% greater izod impact strength than composite specimen SH. The high fracture toughness of the cotton yarn present at the skin layer accounts for this. The izod impact strength rises by 72% over SH when all yarns inside the skin layer are arranged unidirectionally, as in composite specimen WbUD. This is attributable to the improved fracture toughness of composite skin.

Furthermore, the impact strength of the Nw composite is 33% higher than that of the composite specimen SH. This is

Fig. 5 Tensile stress–strain plots (**a**) and flexural stress-deformation plots (**b**) of different composite laminates
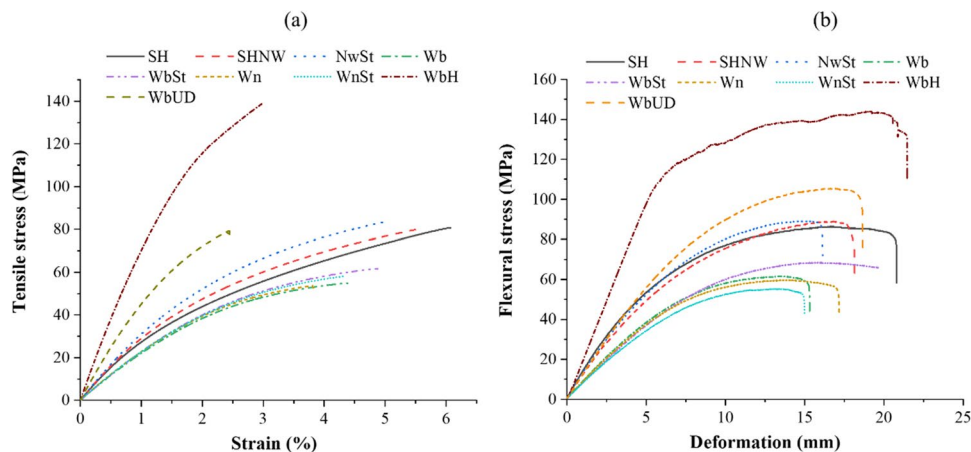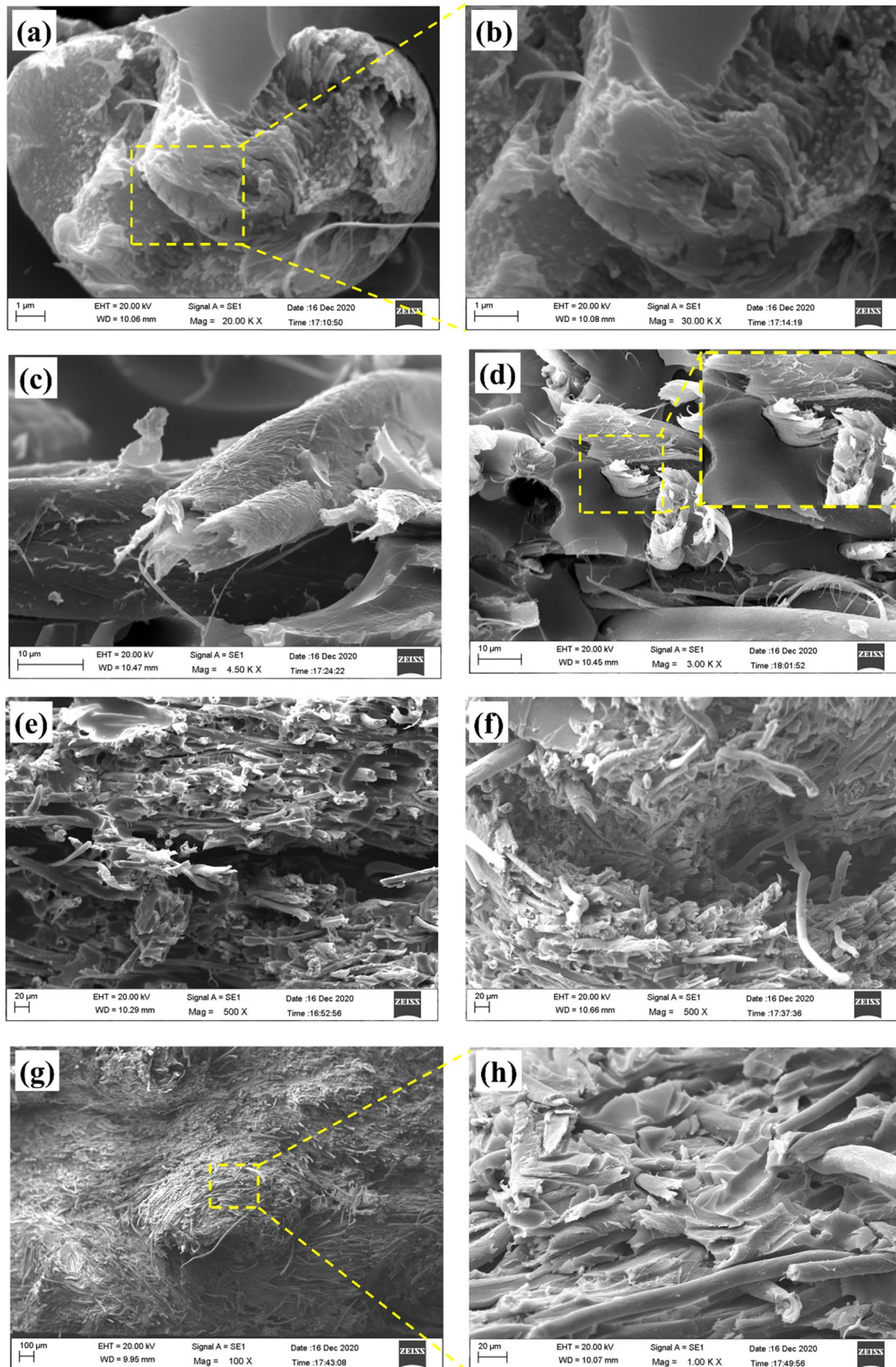
Fig. 6 SEM image of composite specimens SH (**a**, **b**, **c**, and **d**) and Wb (**e**, **f**, **g**, and **h**) fractured under tensile loading
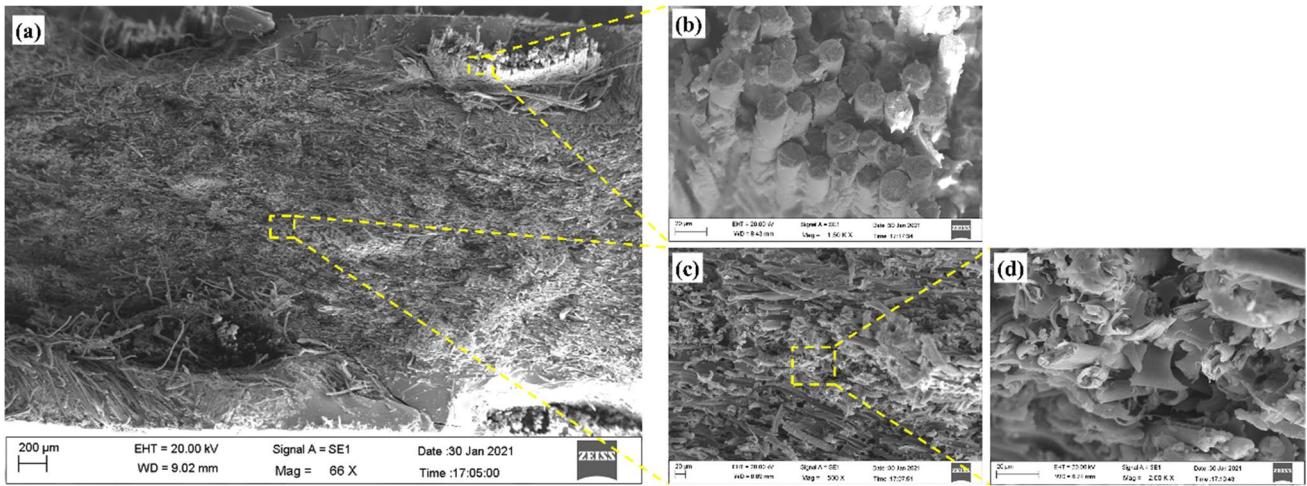
Fig. 7 SEM image of composite specimens Nw (**a**), and Wb (**b**, **c**, and **d**) fractured under tensile loading
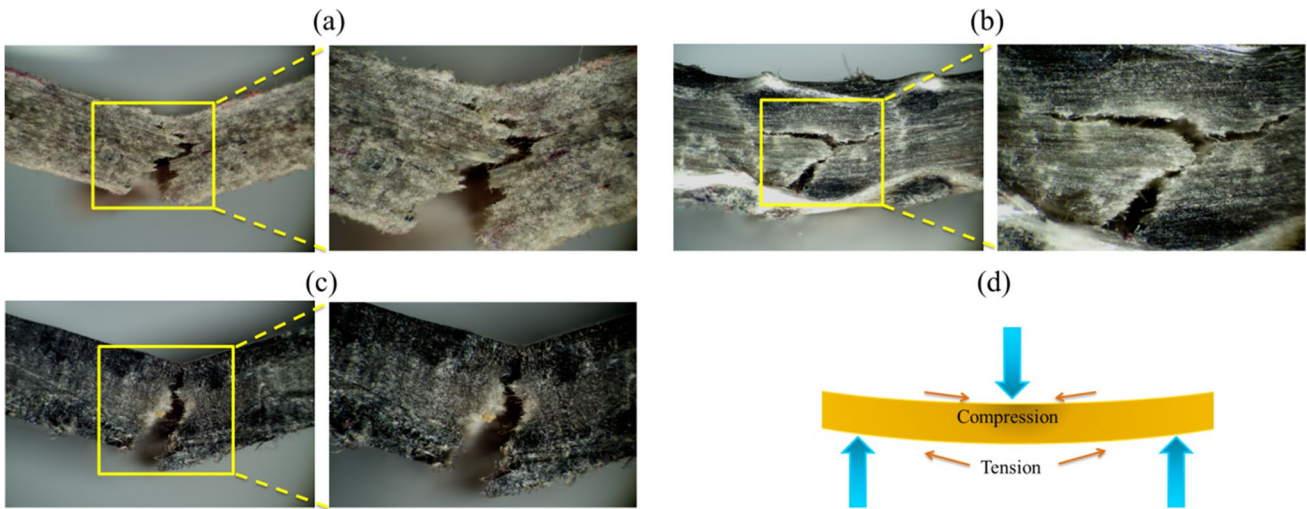

Fig. 8 Flexural fractured SH (**a**), Wb (**b**), and WbH (**c**) specimens

due to needle punching, which causes fibre locking within the preform, resulting in a higher pullout force under impact loading. The impact strength of the composite specimen WbH is 537% greater than that of SH. The high fracture toughness of glass filaments within the skin of composite specimen WbH is responsible for this. The SEM images of impact-fractured composite specimens are shown in Fig. 9. The composite specimens Wb and WbUD show fractured cotton yarn. Also, the cotton fibres at the core of the composites fail due to fibre pullout and fracture. The presence of resin inside the waste cotton yarns indicates its complete wetting.

Understanding the performance of textile waste-reinforced composites under bolted joints is essential for various applications. Further, bolted joints can tolerate environmental effects better than adhesive joints [28]. Figure 10a shows
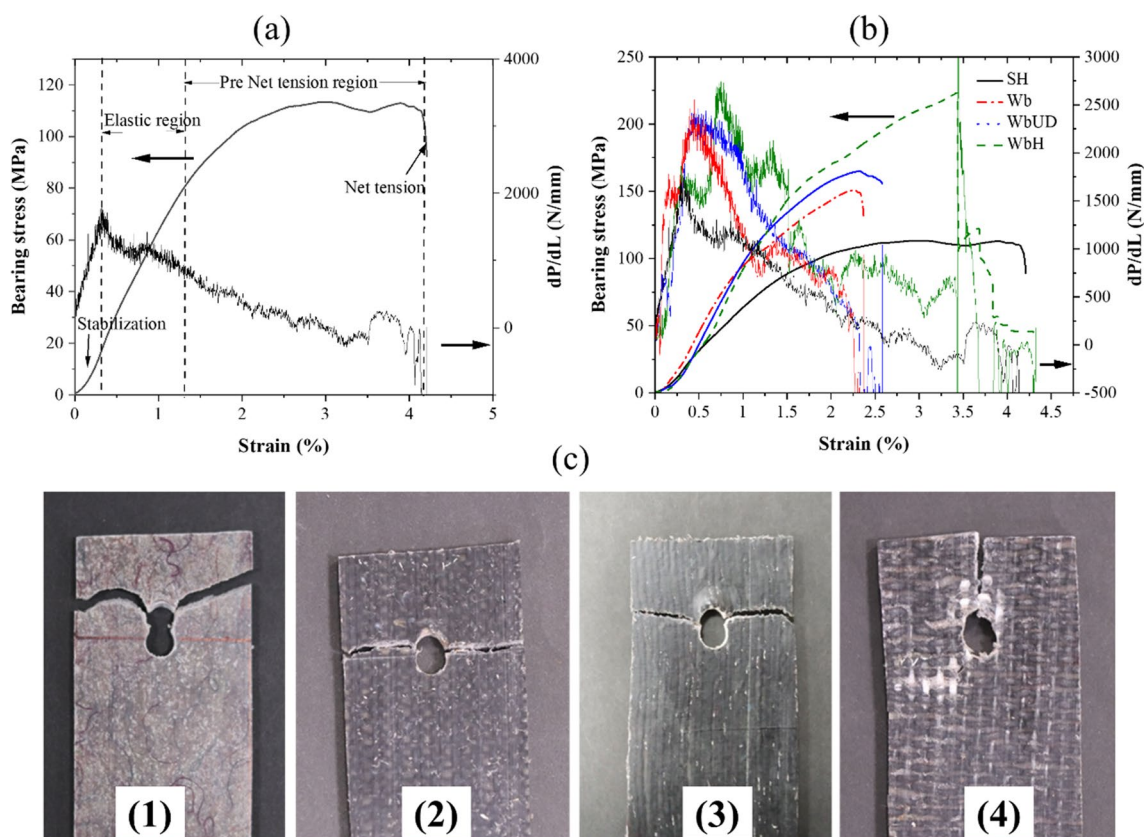
composite specimen SH's bearing strain versus bearing stress plot and dP/dL (load/displacement slope). The stabilising, elastic, and non-elastic regions of the bearing stress/strain curve are followed by a fracture in net tension mode (Fig. 10c1). Joint stiffness is associated with the strain in the elastic zone of composite specimen SH, which ranges from 0.3 to 1.3. At a strain of 0.3%, the maximum value of dP/dL is obtained in this area. The linearity of the curve is observed until local matrix failure occurs, causing a reduction in the dP/dL slope. Between a strain value of 1.3 and 4.15%, the dP/dL slope falls further, showing the non-linear response of the bearing stress–strain curve. The 'pre-net tension zone' is the term given to this area. Matrix crack extension causes local fibre-matrix debonding in the pre-net tension zone which is related to matrix crack extension. The elastic region for composite specimens Wb, WbUD, and WbH is
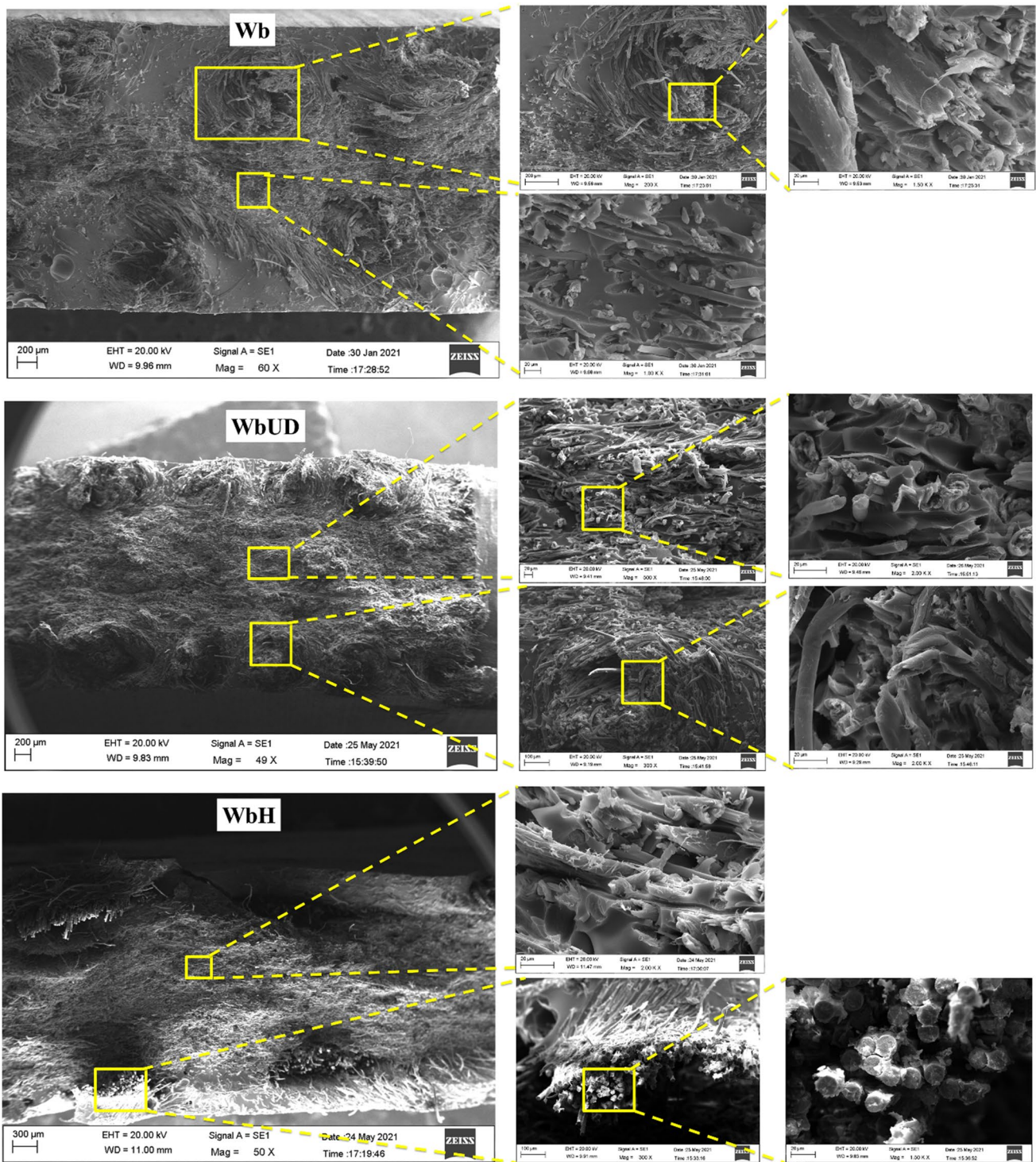
Fig. 9 SEM images of izod impact–fractured composite specimens Wb, WbUD, and WbH

from strain values of 0.25 to 0.81, 0.35 to 0.92, and 0.59 to 1.1%, respectively (Fig. 10b). In this region, the maximum dP/dL slop value is reached at a strain value of 0.45, 0.48, and 0.75% for composite specimens Wb, WbUD, and WbH, respectively. The slope of the dP/dL curve decreases as matrix crack formation starts. The matrix cracking causes the non-linearity of the bearing stress–strain curve. This non-linear region continues until composites fail. The pre-net tension region is less for composite specimen Wb than SH. This is attributed to the higher weight percentage of the

Fig. 10 Plot of bearing stress and load/displacement slope (dP/dL) showing different regions (**a**), trend of bearing stress versus strain for different composites (**b**), and optical images of composite specimens SH (**1**), Wb (**2**), WbUD (**3**), and WbH (**4**) fractured in double-lap pinned joint (**c**)

woven preform in the composite specimen Wb (cotton yarn has lower tensile strength).

Composite specimen Wb has a bearing stress value that is 23% greater than specimen SH. Cotton yarn prevents fracture growth perpendicular to the loading direction. In contrast, the specimen SH has randomly oriented fibres, and the bearing crack grows with the strength of SH being less than Wb. However, the crack propagation in SH is delayed due to the random fibre arrangement. Due to high-strength glass fibres in the loading direction, the bearing stress of WbH is 97% higher than SH, limiting matrix crack formation.

3.2 Thermogravimetric analysis

The thermal response of SH, Wb, and WbH composite was studied using a thermogravimetric analyser. Wb, WbSt, Wn, WnSt, and WbUD composite specimens are all made of the same material. Therefore, only composite specimen Wb was used to represent all of them. Similarly, composite specimens SH and Nw and NwSt have the same composition. The temperature versus weight (%) graphs of various composites are shown in Fig. 11a. Three weight-loss regions can be seen in the TGA plots. From room temperature to 300 °C, there is

a progressive loss of weight. From 300 to 450 °C, structural deterioration of the component materials causes the greatest weight loss. The third temperature range is between 450 and 600 °C when weight loss and char formation occur.

Weight reduction seen till 100 °C relates to moisture elimination from composites [29]. Cellulose decomposes at temperatures ranging from 255 to 340 °C [30]. The cotton fibre's major weight loss was observed in the temperature range of 300 to 400 °C. The $T_{5\%}$ weight loss temperature of the WbH composite specimen is greater than the $T_{5\%}$ weight loss temperature of the SH and Wb composite specimens. Composite specimen WbH has a $T_{5\%}$ that is 16.1% greater than composite specimen SH. This is due to the greater pyrolysis temperature of glass fibres than cotton fibres. Furthermore, the WbH composite specimen has a larger char output at 600 °C than the composite SH. This is due to the cellulose's thermal breakdown at temperatures between 255 and 340 °C [30], whereas the glass fibre's pyrolysis occurs in the temperature range of 600 to 800 °C [31]. The $T_{5\%}$ of composite specimen Wb is ~13.5% higher than SH. This can be attributed to impurities within the waste cotton yarn (such as fibres other than cotton and dyes within the fibres), evidenced by the higher char yield of Wb. The maximum
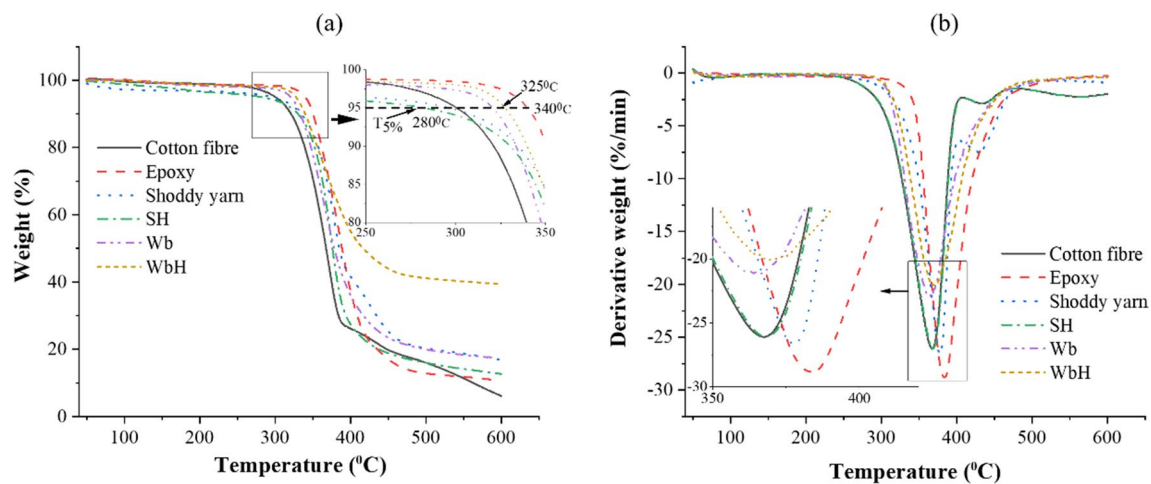
Fig. 11 TGA (**a**) and DTGA (**b**) plots of different composite materials

Table 5 $T_{5\%}$ (°C) and char yield (%) of different materials

Specimen	$T_{5\%}$ (°C)	Char yield (%)
Cotton fibre	301 ± 15	6.1 ± 0.56
Cotton shoddy yarn	294 ± 11	16.82 ± 1.4
Epoxy	340 ± 10	10.63 ± 0.76
SH	282 ± 9	12.65 ± 0.35
Wb	320 ± 5	17.43 ± 0.78
WbH	325 ± 7	40 ± 1.2

weight loss rate for composite specimen WbH is lower than SH and Wb (Fig. 11b). This is due to the greater glass fibre pyrolysis temperature in WbH compared to only cotton fibres in SH and Wb. The $T_{5\%}$ and char yields of various composites are shown in Table 5.

3.3 Water absorption behaviour of the composites

The composite's water absorption behaviour changes with fibre type, orientation, composite thickness, the direction of water diffusion (through the thickness, in the fibre direction), etc. [32]. Water wicking through composites is dependent on the number of fibre-to-fibre interactions [33]. A water-wicking model for short-fibre reinforced composites based on Wang et al.'s [34] water-wicking model for natural fibre composites is shown in Fig. 12b. Further, the fibre at the surface and edges of the composite absorbs the water, resulting in the swelling of these fibres, which causes matrix cracks through which the water penetrates the composite. The composite's different water absorption properties are shown in Table 6. The equilibrium water absorption of composite specimen SH is found to be higher than Wb. This is because woven preform makes approximately 72% of the overall weight of the reinforcement in a composite. This mass is

confined within the yarns, and they are connected only at the interlacement point. Therefore, the water diffusion rate of composite specimen Wb is lower than SH. Further, ~ 36% of the reinforcement's total weight within the composite specimen WbH consists of glass yarn, which has a hydrophobic nature. Therefore, the water diffusion rate of WbH is lower than SH and Wb. Figure 12a depicts the weight gain of various composites over time.

3.4 Comparative analysis of mechanical properties of composites

The density, Young's modulus, and tensile strength of a composite intended for use as a dashboard panel in an automobile must all be more than 1.18 gm/cm³, 2.3 GPa, and 25 MPa, respectively [35]. The mechanical properties of the composites produced in this study are greater than those needed for dashboard panels in an automobile. As a result, these composites might be used in dashboard panels for automobiles and also as non-structural components. Furthermore, the mechanical characteristics of some produced composites are compared to typical values for automotive applications (Table 4S (Supplementary material)). The textile waste-based composites could be potential materials for use in interior furniture components of public transport buses and trains.

Mechanical characteristics of the produced composite were similar to those of industrial particleboard, medium-density fibreboard, and rubberwood epoxy composite [36]. Table 5S (Supplementary material) lists the mechanical parameters of P1, P2, P4, and P6 particleboards, which are utilised in various applications. All developed composites have more excellent tensile and flexural moduli than are required for disparate particleboard applications. They can also be used as top and bottom skins to make laminated
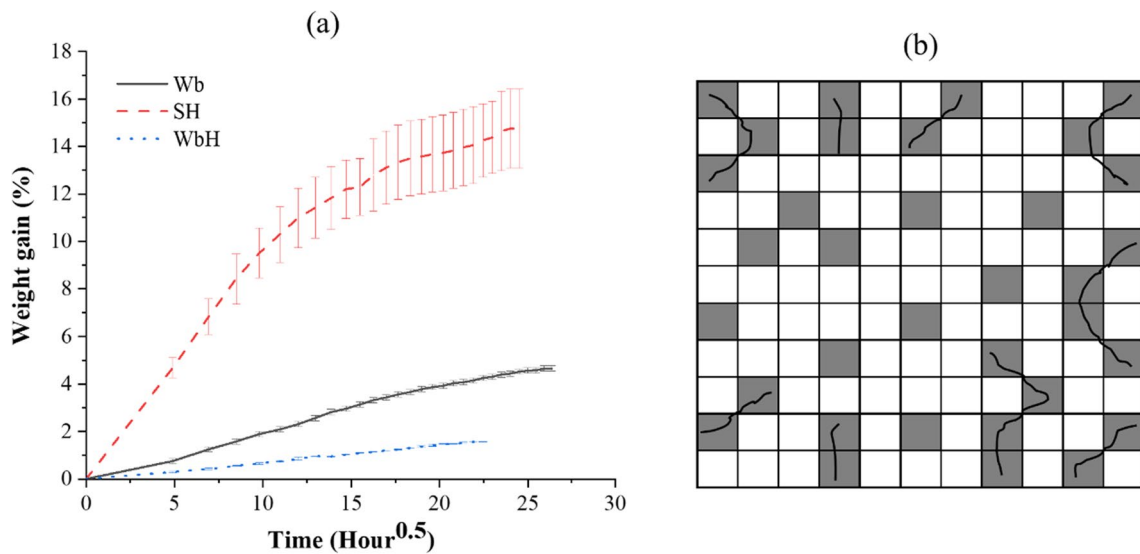
Fig. 12 Weight gain with time plot of different composite specimens (**a**) and model of water wicking through the composite (**b**)

Table 6 Water absorption characteristics of composites

Specimen	M_∞ (%)	Diffusion rate (%.hr^{-1})	$D \times 10^{-6}$ (mm^2.sec^{-1})	θ (%.h$^{-0.5}$)	WTR (g.m^{-2}.day^{-1})	S (g/g)	$P \times 10^{-7}$ (m^2.sec^{-1})
SH	14.75 ± 1	0.025 ± 0.005	1.5 ± 0.23	0.852 ± 0.15	7.60 ± 0.9	0.147 ± 0.03	2.20 ± 0.1
Wb	4.68 ± 0.6	0.007 ± 0.001	0.78 ± 0.1	0.2 ± 0.05	2.48 ± 0.2	0.05 ± 0.004	0.36 ± 0.04
WbH	1.57 ± 0.2	0.003 ± 0.001	0.65 ± 0.07	0.1 ± 0.05	1.82 ± 0.35	0.016 ± 0.002	0.1 ± 0.03

composite FRS structures that are used in building and construction materials.

4 Conclusions

Engineering the preform structure can improve the mechanical characteristics of recycled cotton carded web-reinforced composites. Compared to SH, the composite specimens Nw, NwSt, Wb, WbSt, Wn, and WnSt exhibit no marked improvement in tensile and flexural properties. The izod impact strength of composite specimens, namely Wb, Wn, WbSt, and WnSt, increases by 40% when the woven fabric is placed on the skin. Flexural and impact strength are increased by 26 and 72%, respectively, in the composite specimen WbUD. Its tensile strength, on the other hand, was similar to SH. The WbH outperforms the SH in terms of tensile, flexural, and izod impact strength by 74, 68, and 537%, respectively, due to high-strength glass yarn in the loading direction. WbUD and WbH composite specimens had lower-bearing stress in the double-lap pinned joint than SH. Furthermore, because of the high pyrolysis temperature of the glass yarn, the WbH exhibit superior thermal

degradation behaviour than the other composites. All of the composites produced, however, are thermally stable. WbUD and WbH have lower equilibrium water content and diffusion rates than SH. Textile waste-reinforced composites are promising materials for automotive, building, and construction applications. A great amount of research is still needed to optimise the preform structures and composite manufacturing technologies to further reduce the environmental impact during and after recycling.

Declarations

Ethics approval and consent to participate Not applicable.

Consent for publication Not applicable.

Competing interests The authors declare no competing interests.

References

1. Milburn J (2016) The numbers on textile waste. https://textilebeat.com/the-numbers-on-textile-waste/. Accessed 30 May 2021

2. Kerr J, Landry J (2017) Pulse of the fashion industry. Global Fashion Agenda & The Boston Consulting Group

3. Umar M, Shaker K, Ahmad S et al (2017) Investigating the mechanical behavior of composites made from textile industry waste. J Text Inst 108:835–839. https://doi.org/10.1080/00405000.2016.1193982

4. Wang Z, Yao ZJ, Zhou J, Zhang Y (2017) Reuse of waste cotton cloth for the extraction of cellulose nanocrystals. Carbohydr Polym 157:945–952. https://doi.org/10.1016/j.carbpol.2016.10.044

5. Khan A, Awais M, Mohsin M (2023) Recycling textile waste into innovative carbon black and applications to smart textiles: a sustainable approach. Biomass Convers Biorefinery. https://doi.org/10.1007/s13399-023-04475-4

6. Dissanayake DGK, Weerasinghe DU (2021) Fabric waste recycling: a systematic review of methods, applications, and challenges. Mater Circ Econ 3:24. https://doi.org/10.1007/s42824-021-00042-2

7. Zhang Z, Rumi SS, Lucia LA, Abidi N (2023) Waste treat waste: alginate calcium versus alginate acid gels in upcycling waste cotton linter as composite biosorbent. Ind Crops Prod 205:117512. https://doi.org/10.1016/j.indcrop.2023.117512

8. Ramamoorthy SK, Skrifvars M, Alagar R, Akhtar N (2018) End-of-life textiles as reinforcements in biocomposites. J Polym Environ 26:487–498. https://doi.org/10.1007/s10924-017-0965-x

9. Temmink R, Baghaei B, Skrifvars M (2018) Development of bio-composites from denim waste and thermoset bio-resins for structural applications. Compos Part A Appl Sci Manuf 106:59–69. https://doi.org/10.1016/j.compositesa.2017.12.011

10. Achukwu E, Owen M, Danladi A et al (2023) Recycling effects on the bending, rheological, and structural properties of glass fiber-reinforced isotactic polypropylene composites. J Reinf Plast Compos 073168442311675. https://doi.org/10.1177/07316844231167552

11. Owen MM, Achukwu EO, Romli AZ et al (2023) Thermal and mechanical characterization of composite materials from industrial plastic wastes and recycled nylon fibers for floor paving tiles application. Waste Manag 166:25–34. https://doi.org/10.1016/j.wasman.2023.04.038

12. Owen MM, Achukwu EO, Anjang Ab Rahman A, et al (2023) Mechanical and morphological characterizations of epoxy composites reinforced with surface modified woven cotton structures using vacuum bagging technique. J Text Inst 1–15. https://doi.org/10.1080/00405000.2023.2258047

13. Owen MM, Achukwu EO, Akil HM et al (2022) Effect of epoxy concentrations on thermo-mechanical properties of kenaf fiber – recycled poly (ethylene terephthalate) composites. J Ind Text 52:152808372211274. https://doi.org/10.1177/15280837221127441

14. Singh AAMM, Franco PA, Azhagesan N, Sharun V (2023) Exploring seashell and rice husk waste for lightweight hybrid biocomposites: synthesis, microstructure, and mechanical performance. Biomass Convers Biorefinery. https://doi.org/10.1007/s13399-023-04846-x

15. Hangargi S, Swamy A, Raj RG et al (2023) Enhancement of Kevlar fiber-polypropylene composite by the inclusions of cotton stalk and granite particle: characteristics study. Biomass Convers Biorefinery. https://doi.org/10.1007/s13399-023-04817-2

16. Jagadeesan R, Suyambulingam I, Divakaran D, Siengchin S (2023) Novel sesame oil cake biomass waste derived cellulose micro-fillers reinforced with basalt/banana fibre-based hybrid polymeric composite for lightweight applications. Biomass Convers Biorefinery 13:4443–4458. https://doi.org/10.1007/s13399-022-03570-2

17. Meng X, Fan W, Ma Y et al (2020) Recycling of denim fabric wastes into high-performance composites using the needle-punching nonwoven fabrication route. Text Res J 90:695–709. https://doi.org/10.1177/0040517519870317

18. Baccouch W, Ghith A, Yalcin-Enis I et al (2020) Investigation of the mechanical, thermal, and acoustical behaviors of cotton, polyester, and cotton/polyester nonwoven wastes reinforced epoxy composites. J Ind Text 51(6):876–99. https://doi.org/10.1177/1528083720901864

19. Khurshid MF, Hengstermann M, Hasan MMB et al (2019) Recent developments in the processing of waste carbon fibre for thermoplastic composites – a review. J Compos Mater 54:1925–1944. https://doi.org/10.1177/0021998319886043

20. Frydrych I, Ahmad S, Umair M et al (2018) Mechanical behaviour of hybrid composites developed from textile waste. Fibres Text East Eur 26:46–52. https://doi.org/10.5604/01.3001.0010.7796

21. Kamble Z, Behera BK (2021) Upcycling textile wastes: challenges and innovations. Text Prog 53:65–122. https://doi.org/10.1080/00405167.2021.1986965

22. Wanassi B, Azzouz B, Ben HM (2016) Value-added waste cotton yarn: Optimization of recycling process and spinning of reclaimed fibers. Ind Crops Prod 87:27–32. https://doi.org/10.1016/j.indcrop.2016.04.020

23. Kamble Z, Behera BK (2020) Mechanical properties and water absorption characteristics of composites reinforced with cotton fibres recovered from textile waste. J Eng Fiber Fabr 15:1–8. https://doi.org/10.1177/1558925020901530

24. Roy R, Ishtiaque S, Dixit P (2020) Impact of fibre orientation on thickness and tensile strength of needle-punched nonwoven: optimization of carding parameters. J Ind Text 51:4801S–17S. https://doi.org/10.1177/1528083720910706

25. Ahmed KS, Vijayarangan S (2008) Tensile, flexural and interlaminar shear properties of woven jute and jute-glass fabric reinforced polyester composites. J Mater Process Technol 207:330–335. https://doi.org/10.1016/j.jmatprotec.2008.06.038

26. Lee H, Kureemun U, Ravandi M, Teo WS (2020) Performance of interlaminar flax-carbon hybrids under bending. Procedia Manuf 43:658–665. https://doi.org/10.1016/j.promfg.2020.02.134

27. Jawaid M, Abdul Khalil HPS, Abu Bakar A (2010) Mechanical performance of oil palm empty fruit bunches/jute fibres reinforced epoxy hybrid composites. Mater Sci Eng A 527:7944–7949. https://doi.org/10.1016/j.msea.2010.09.005

28. Fiore V, Calabrese L, Scalici T et al (2018) Experimental design of the bearing performances of flax fiber reinforced epoxy composites by a failure map. Compos Part B Eng 148:40–48. https://doi.org/10.1016/j.compositesb.2018.04.044

29. Ahmad MAA, Majid MSA, Ridzuan MJM et al (2018) Dynamic mechanical analysis and effects of moisture on mechanical

properties of interwoven hemp/polyethylene terephthalate (PET) hybrid composites. Constr Build Mater 179:265–276. https://doi.org/10.1063/1.5066678

30. Silva CG, Benaducci D, Frollini E (2012) Lyocell and cotton fibers as reinforcements for a thermoset polymer. BioResources 7:78–98

31. Chinnasamy V, Subramani SP, Palaniappan SK et al (2020) Characterization on thermal properties of glass fiber and kevlar fiber with modified epoxy hybrid composites. J Mater Res Technol 9:3158–3167. https://doi.org/10.1016/j.jmrt.2020.01.061

32. Chilali A, Assarar M, Zouari W et al (2017) Effect of geometric dimensions and fibre orientation on 3D moisture diffusion in flax fibre reinforced thermoplastic and thermosetting composites. Compos Part A Appl Sci Manuf 95:75–86. https://doi.org/10.1016/j.compositesa.2016.12.020

33. Mahalingam J (2022) Mechanical, thermal, and water absorption properties of hybrid short coconut tree primary flower leaf stalk fiber/glass fiber-reinforced unsaturated polyester composites for biomedical applications. Biomass Convers Biorefinery. https://doi.org/10.1007/s13399-022-02958-4

34. Wang W, Sain M, Cooper PA (2006) Study of moisture absorption in natural fiber plastic composites. Compos Sci Technol 66:379–386. https://doi.org/10.1016/j.compscitech.2005.07.027

35. Kamble Z, Behera BK (2021) Fabrication and performance evaluation of waste cotton and polyester fiber-reinforced green composites for building and construction applications. Polym Compos 42:3025–3037. https://doi.org/10.1002/pc.26036

36. Prakash V, Bera T, Acharya SK (2019) Mechanical and erosive wear behavior of rubber wood particulate reinforced epoxy composite. Mater Today Proc 19:223–227. https://doi.org/10.1016/j.matpr.2019.06.708